AD-A106 281 ELECTRONICS RESEARCH LAB ADELAIDE (AUSTRALIA) F/G 20/14
FIELD-ALIGNED IONIZATION SCATTER GEOMETRY APPLIED TO TRANSEQUAT--ETC(U)
AUG 80 K B PARCELL
UNCLASSIFIED ERL-0158-TR NL

AD A106281

END
DATE
FILMED
11 81
DTIC

(12)

ERL-0158-TR

AR-002-035

AD A106281

DEPARTMENT OF DEFENCE

DEFENCE SCIENCE AND TECHNOLOGY ORGANISATION

ELECTRONICS RESEARCH LABORATORY

DEFENCE RESEARCH CENTRE SALISBURY
SOUTH AUSTRALIA

TECHNICAL REPORT

ERL-0158-TR

FIELD-ALIGNED IONIZATION SCATTER GEOMETRY
APPLIED TO TRANSEQUATORIAL PATHS

K.B. PARCELL

Approved for Public Release

COPY No. 45

AUGUST 1980

UNCLASSIFIED

AR-002-035

DEPARTMENT OF DEFENCE

DEFENCE SCIENCE AND TECHNOLOGY ORGANISATION

ELECTRONICS RESEARCH LABORATORY

TECHNICAL REPORT

ERL-0158-TR

FIELD-ALIGNED IONIZATION SCATTER GEOMETRY APPLIED TO TRANSEQUATORIAL PATHS

K.B. Parcell

S U M M A R Y

The mathematical description of the geometry for forward specular scattering of radio waves by field-aligned ionization irregularities has been extended to cover transequatorial ray paths. The equations presented include expressions for paths involving either one scattering point in the same geomagnetic hemisphere as the transmitter, or two scattering points, one on each side of the geomagnetic equator.

POSTAL ADDRESS: Chief Superintendent, Electronics Research Laboratory
Box 2151, G.P.O., Adelaide, South Australia, 5001

UNCLASSIFIED

TABLE OF CONTENTS

		Page No.
1.	INTRODUCTION	1
2.	PREVIOUS SINGLE SCATTERING POINT GEOMETRY	2 - 4
3.	APPLICATION IN THE SOUTHERN HEMISPHERE	4 - 5
4.	TRANSEQUATORIAL SCATTERED RAY PATHS	5 - 10
5.	CONCLUDING REMARKS	10 - 11
	REFERENCES	12

LIST OF FIGURES

1. Propagation angle, geometric configuration
2. Auroral scattering geometry
3. Scatter geometry in the southern geomagnetic hemisphere
4. Transequatorial scatter geometry

1. INTRODUCTION

Magnetic field-aligned ionization has been detected in the ionosphere for many years and by several experimental techniques. Such irregularities are most prevalent in the auroral region but have also been found to exist at low latitudes (refs. 1, 2). The generally accepted form of the ionization irregularities is of a tube or column of increased or depleted electron density confined and elongated along a magnetic field line. Radio waves incident on magnetic field-aligned ionization in a direction perpendicular to the magnetic field lines are scattered back in the direction of incidence, a property which has formed the basis for most experimental investigation of the phenomenon.

In addition to this aspect-sensitive scattering, incident radiation can undergo forward scattering when the direction of propagation makes an angle of other than 90° with the magnetic field lines. Experimental observations have demonstrated that forward scattering is specular or nearly specular, i.e. the angle of scatter (or reflection) is equal to the angle of incidence. Thus the scattered signal describes a conical surface surrounding the column of ionization, which is consistent with a theory for scattering of radio waves by field-aligned ionization proposed by Booker (ref. 3).

Two previous mathematical developments of forward scatter geometry by Leadabrand and Yarbroff (ref. 4) and Millman (refs. 5, 6) used the specular reflection condition. Both treatments were confined to a single scattering point in the northern geomagnetic hemisphere, Leadabrand and Yarbroff using plane earth geometry while Millman included the curvature of the earth by using a spherical co-ordinate system.

In order to apply the scatter geometry as a possible explanation of VHF radio propagation over transequatorial paths, Millman's equations have been checked for applicability to specular scattering in either geomagnetic hemisphere. In addition, the present treatment includes paths which involve two scattering irregularities in the ionosphere, one on either side of the geomagnetic equator. Transequatorial paths can thus be calculated for radio waves which are scattered at either one or two ionospheric points before returning to the surface of the earth.

2. PREVIOUS SINGLE SCATTERING POINT GEOMETRY

The first step is to introduce the equations given by Millman (ref. 5) and verify their applicability to the southern geomagnetic hemisphere. For the most part, the notation will follow that of Millman or will be a logical extension of it.

Millman defines the angle between the direction of the magnetic field line and the direction of electromagnetic propagation at the scattering point as the propagation angle θ. This is illustrated in figure 1 taken from Millman (ref. 5).

The various symbols refer to the following:

- P_S the scattering point in space
- P_G the point vertically beneath P_S on the earth's surface
- R slant range from the transmitter location to P_S
- I magnetic inclination angle (or dip) at point P_S
- a the point of intersection of the direction of electromagnetic propagation with the plane tangent to the earth's surface at P_G
- b the point of intersection of the direction of the magnetic field line which passes through P_S
- $\overline{P_G b}$ line in the tangent plane whose orientation coincides with a meridian of geomagnetic longitude
- α azimuth bearing of the transmitter location with respect to P_G
- e angle formed by the intersection of the propagation vector and the vertical connecting P_S and P_G (NB: the latter is a radial from the centre of the earth)
- r_o radius of the earth.

Millman considers the two triangles aP_Sb and aP_Gb to obtain from the law of cosines,

$$\overline{ab}^2 = \overline{aP_S}^2 + \overline{bP_S}^2 - 2\,\overline{aP_S}.\overline{bP_S}\cos(180 - \theta) \tag{1}$$

and

$$\overline{ab}^2 = \overline{aP_G}^2 + \overline{bP_G}^2 - 2\,\overline{aP_G}.\overline{bP_G}\cos\alpha \quad . \tag{2}$$

Equating the two expressions, it follows that

$$h^2 + 2\,\overline{aP_S}.\overline{bP_S}\cos\theta = -h^2 - 2\,\overline{aP_G}.\overline{bP_G}\cos\alpha \quad , \qquad (3)$$

where

$$h^2 = \overline{P_S P_G}^2 = \overline{aP_S}^2 - \overline{aP_G}^2 = \overline{bP_S}^2 - \overline{bP_G}^2 \quad . \qquad (4)$$

Since

$$\sin e = \frac{\overline{aP_G}}{\overline{aP_S}} \qquad \cos e = \frac{h}{\overline{aP_S}}$$

$$\sin I = \frac{h}{\overline{bP_S}} \qquad \cos I = \frac{\overline{bP_G}}{\overline{bP_S}} \quad ,$$

equation (3) simplifies to

$$\cos\theta = -\cos e \sin I - \sin e \cos I \cos\alpha \quad . \qquad (5)$$

Millman then specifies the angles e, I and α in terms of known parameters to solve for θ. The parameters he assumes are λ_R and ϕ_R, the geographic longitude and latitude of the transmitter site and the co-ordinates of point P_S with respect to that location; A, E and h. He derives the magnetic field quantities I and α from an earth-centred dipole model of the field with the geomagnetic north pole at geographic longitude λ_M and latitude ϕ_M.

The inclination, or magnetic dip I, specifies the direction of the total magnetic intensity vector with respect to the horizontal and, by definition, is measured positively in the downward direction. For a dipole field model, it is a function only of geomagnetic latitude defined by

$$I = \tan^{-1}(2\tan\psi_P) \quad , \qquad (6)$$

where ψ_P is the geomagnetic latitude of both points P_S and P_G and can be expressed in terms of geographic co-ordinates ϕ_P, λ_P.

$$\psi_P = \sin^{-1}\{\cos(\lambda_M - \lambda_P)\cos\phi_M \cos\phi_P + \sin\phi_M \sin\phi_P\} \qquad (7)$$

In Millman's later paper (ref. 6) he defines α by the equation

$$\alpha = \gamma - D \quad , \qquad (8)$$

where

γ is the geographic azimuth (bearing) of the transmitter location with respect to P_G and

D is the local magnetic declination (or variation).

Both of these may be expressed in terms of geographic co-ordinates

$$\gamma = \tan^{-1}\left[\frac{\sin(\lambda_R - \lambda_P)\cos\phi_R}{\sin\phi_R \cos\phi_P - \cos\phi_R \sin\phi_P \cos(\lambda_R - \lambda_P)}\right] \tag{9}$$

$$D = \tan^{-1}\left[\frac{\sin(\lambda_M - \lambda_P)\cos\phi_M}{\sin\phi_M \cos\phi_P - \cos\phi_M \sin\phi_P \cos(\lambda_M - \lambda_P)}\right] \tag{10}$$

the latter expression applying for the dipole field.

Finally, the angle e can be evaluated by the sine rule from the vertical triangle to the earth's centre.

$$e = \sin^{-1}\left[\frac{r_o}{r_o + h}\cos E\right] \tag{11}$$

Having established the incident propagation angle, the direction of propagation after the forward scattering can be determined. As shown in figure 2 taken from reference 6, Millman defines $(\pi - \theta_r)$ as the propagation angle formed by the scattered ray and the magnetic-field line. Thus the condition of specular scatter requires that

$$\cos\theta_r = -\cos\theta \quad . \tag{12}$$

3. APPLICATION IN THE SOUTHERN HEMISPHERE

Figure 3 illustrates the application of the scatter geometry to a point in the southern geomagnetic hemisphere. Some emphasis is placed on the transfer here, since it is not immediately obvious that the previous equations are valid in this situation.

There are two differences from figure 1, associated with the magnetic field. By definition, the dip angle must be negative in the southern hemisphere. In proceeding from equation (3) to equation (4), the absolute value of dip angle was transferred into the triangle bP_GP_S in order to obtain expressions for the functions sine and cosine of I. The same transfer can again be made but the negative sign associated with the dip angle must not be forgotten. The second difference is that the angle bP_Ga is no longer α, but is equal to $(\pi - \alpha)$.

A further change is that the angle at the apex of triangle aP_Sb becomes equal to θ rather than its supplement as before.

Thus the equation (3) is re-written as

$$h^2 - 2\,\overline{aP}_S.\overline{bP}_S \cos\theta = -h^2 + 2\,\overline{aP}_G.\overline{bP}_G \cos\alpha \quad , \qquad (13)$$

which after substitution becomes

$$\cos\theta = \cos e \sin|I| - \sin e \cos|I| \cos\alpha \quad . \qquad (14)$$

Since I will be negative and will lie in the range $-\frac{\pi}{2} < I < 0$, the equation (14) may be converted to

$$\cos\theta = -\cos e \sin I - \sin e \cos I \cos\alpha \quad , \qquad (15)$$

which is exactly the same as equation (5).

4. TRANSEQUATORIAL SCATTERED RAY PATHS

Two types of transequatorial paths are proposed. The first are those families of paths in which the rays undergo forward scattering at a single point and return to the earth's surface in the opposite geomagnetic hemisphere to the transmitter location. The other type include the rays which miss the earth after one forward scattering, but then reach ionospheric heights in the opposite geomagnetic hemisphere. Under appropriate conditions, forward scattering could occur at a second point, whence some of the ray paths would return to the earth's surface at much higher latitudes in the second hemisphere.

It is possible to trace those ray paths which could be transmitted from a certain location ϕ_R, λ_R, and propagate via this mechanism to points in the opposite hemisphere by considering ranges of initial elevation angle E and geographic azimuth bearing ξ. Heights at which the scattering might occur are fixed at h_1 in the transmitting hemisphere and h_2 in the other hemisphere. The angle e between the initial ray path and the zenith at the first point of forward scattering is determined from equation (11), i.e.

$$e = \sin^{-1}\left(\frac{r_o}{r_o + h_1} \cos E\right) \quad . \qquad (16)$$

It follows that the earth centre angle between the transmitter location and the scattering point is

$$\nu = \frac{\pi}{2} - E - e \quad . \tag{17}$$

The co-ordinates of the first scattering point can then be obtained by applying the sine and cosine rules for spherical triangles, viz

$$\phi_P = \sin^{-1}\left(\sin\phi_R \cos\nu + \cos\phi_R \sin\nu \cos\xi\right) \tag{18}$$

and

$$\lambda_P = \lambda_R + \sin^{-1}\left(\frac{\sin\xi \sin\nu}{\cos\phi_P}\right) \quad . \tag{19}$$

The bearing of the transmitter location with respect to the sub-ionospheric point, i.e. the location on the earth's surface directly beneath the first scattering point, will be γ as given by equation (9).

Thus the incident propagation angle θ can be found using equation (3), allowing substitution of equation (8).

$$\theta = \cos^{-1}\left(-\cos e \sin I - \sin e \cos I \cos(\gamma - D)\right) \tag{20}$$

It remains to specify the magnetic field parameters I and D, which may be done simply by the dipole field model as given before, using particular geographic co-ordinates for the north geomagnetic pole, thus

$$\begin{aligned} \lambda_M &= 70.1^\circ \text{ W} \\ \phi_M &= 78.6^\circ \text{ N} \quad . \end{aligned} \tag{21}$$

Alternatively, the magnetic field parameters could be derived during any computation from a spherical harmonic representation of the field such as that of Jensen and Cain (ref. 7). It would also be possible to determine these parameters by interpolation of values scaled from magnetic charts over a suitable grid, having stored the grid values in a matrix for computer reference.

Once the forward scattering has occurred, the scattered signal described a conical surface surrounding the magnetic field line, with the apex at the scattering point. All the scattered rays in the cone have the same propagation angle of $(\pi - \theta_r)$ as defined in figure 2. Depending on the magnetic dip angle, some of the lower part of the cone might intersect the surface of the earth in a smooth curve, while other ray paths can miss the earth and propagate into the opposite hemisphere.

The expression for the scattered propagation angle is similar to equation (20)

$$\cos(\pi - \theta_r) = - \cos e_r \sin I - \sin e_r \cos I \cos(\gamma_r - D) \quad , \qquad (22)$$

where the subscript r refers to the scattered (or reflected) ray.

The equation may be re-arranged to obtain γ_r, which is the azimuth of the scattered rays

$$\gamma_r = \cos^{-1}\left(\frac{\cos\theta_r - \cos e_r \sin I}{\sin e_r \cos I}\right) + D \quad . \qquad (23)$$

Substituting equation (12),

$$\gamma_r = \cos^{-1}\left(\frac{- \cos\theta - \cos e_r \sin I}{\sin e_r \cos I}\right) + D \quad . \qquad (24)$$

The cone is formed by allowing the zenith angle e_r to vary over a range of values from

$$(e_r)_{min} = \left|\frac{\pi}{2} - (I + \theta)\right| \qquad (25)$$

to

$$(e_r)_{max} = (e_r)_{min} + 2\theta \quad . \qquad (26)$$

Both these extremes apply to scattered rays lying in the direction of the magnetic field, vertically below and above the field line. The inverse cosine function of equation (24) may take either a positive or negative value to produce the horizontal spread of the cone on each side of the field line.

The scattered rays which intersect the earth's surface must lie below

$$(e_r)_t = \sin^{-1}\left(\frac{r_o}{r_o + h_1}\right) \quad , \qquad (27)$$

which is the condition of tangency with the earth.

If $(e_r)_{min}$ is less than $(e_r)_t$, then part of the cone will intersect the earth's surface and the location at which the rays reach the surface may be calculated.

The earth centre angle between the scattering point and each earth intersection point is given by β_r.

$$\beta_r = \sin^{-1}\left(\frac{r_o + h_1}{r_o} \sin e_r\right) - e_r \tag{28}$$

The geographic co-ordinates of these points are then

$$\phi_r = \sin^{-1}\left(\sin\phi_p \cos\beta_r + \cos\phi_p \sin\beta_r \cos\gamma_r\right) \quad , \tag{29}$$

$$\lambda_r = \lambda_p + \sin^{-1}\left(\frac{\sin\beta_r \sin\gamma_r}{\cos\phi_r}\right) \quad . \tag{30}$$

The scattered rays in the cone, which will be forward scattered a second time at the appropriate height in the opposite hemisphere, can now be considered. Figure 4 introduces the notation to be used by illustrating a transequatorial ray path lying in the geomagnetic longitude meridian plane of the simple dipole field model. Similar subscripts are used but the prime (′) indicates relation to the second scattering point.

The second scatter point is determined by the triangle with its base from the first to the second scatter point and its apex at the centre of the earth. It is thus possible to transpose to the second scatter point using

$$e' = \sin^{-1}\left(\frac{r_o + h_1}{r_o + h_2} \sin e_r\right) \quad . \tag{31}$$

From the same triangle, the earth centre angle between the two scatter points is

$$\omega = \pi - e_r - e' \tag{32}$$

and bearing from the first to the second is γ_r as given in equation (24). Thus

$$\phi'_p = \sin^{-1}\left(\sin\phi_p \cos\omega + \cos\phi_p \sin\omega \cos\gamma_r\right) \tag{33}$$

and

$$\lambda'_p = \lambda_p + \sin^{-1}\left(\frac{\sin\omega \sin\gamma_r}{\cos\phi'_p}\right) \quad . \tag{34}$$

The range of values of e_r which will produce such ray paths begins at the tangency condition of equation (27), with the upper limit occurring when the ray path reaches the second scattering height at the geomagnetic equator.

If the dipole field relation

$$\psi_p = \tan^{-1}(\tfrac{1}{2} \tan I) \tag{35}$$

is assumed for any field model, the upper limit can be expressed by the implicit relation

$$\frac{r_o + h_1}{r_o + h_2} \sin e_r \geq \sin(\psi_p + e_r) \quad . \tag{36}$$

A number of second scatter points will be found and, for each location (ϕ_p', λ_p'), the appropriate magnetic field parameters determined. These are substituted in an expression for the second incident propagation angle θ'.

$$\theta' = \cos^{-1}\left(- \cos e' \sin I' - \sin e' \cos I' \cos(\gamma' - D')\right) \quad . \tag{37}$$

where D' is the magnetic declination at the second scatter point and

γ' is the bearing of the first scatter point with respect to the second.

$$\gamma' = \tan^{-1}\left(\frac{\sin(\lambda_p - \lambda_p') \cos\phi_p}{\sin\phi_p \cos\phi_p' - \cos\phi_p \sin\phi_p' \cos(\lambda_p - \lambda_p')}\right) \tag{38}$$

The azimuth bearing of the ray paths after a second forward scattering is given by

$$\gamma_r' = \cos^{-1}\left(\frac{- \cos\theta' - \cos e_r' \sin I'}{\sin e_r' \cos I'}\right) + D' \quad . \tag{39}$$

Therefore, at each of the possible second scatter points new cones of rays will be produced, some of which will intersect the earth's surface to form sets of smooth arcs.

The limits on values e_r' may take are

$$(e_r')_{min} = \left|\frac{\pi}{2} - (\theta' + I')\right| \tag{40}$$

and

$$(e_r')_t = \sin^{-1}\left(\frac{r_o}{r_o + h_2}\right) \quad . \tag{41}$$

Finally, the sets of earth centre angles between the second scatter points and the earth intersection points of their conical scatter surfaces are

$$\beta_r' = \sin^{-1}\left(\frac{r_o + h_2}{r_o} \sin e_r'\right) - e_r' \quad , \qquad (42)$$

which leads to the general expressions for the geographic co-ordinates of these intersections

$$\phi_r' = \sin^{-1}\left(\sin\phi_p' \cos\beta_r' + \cos\phi_p' \sin\beta_r' \cos\gamma_r'\right) \qquad (43)$$

and

$$\lambda_r' = \lambda_p' + \sin^{-1}\left(\frac{\sin\beta_r' \sin\gamma_r'}{\cos\phi_r'}\right) \quad . \qquad (44)$$

5. CONCLUDING REMARKS

The mathematical description of field-aligned ionization scatter geometry, originally derived by Millman (refs. 5, 6) for forward scattering of radio waves, has been extended to include transequatorial paths.

Mathematical expressions have been derived which will enable the calculation of ray paths from a transmitter in one geomagnetic hemisphere to points on the surface of the earth in the other hemisphere, where the mode of propagation has been by means of forward specular scattering.

There can be two types of transequatorial scattered ray paths. The first undergo forward scattering at a point in the same hemisphere as the transmitter, but return to ground as the lower portion of the scattered ray cone, the geographic co-ordinates of the resulting arc of intersection being given by equations (29) and (30). The other type of path arises from the two arcs of the same scatter cone horizontally on each side of the central field line, which miss the earth, but intersect the ionosphere in the opposite hemisphere to produce a set of second scattering points. Each of these in turn results in a cone of scattered ray paths, part of which may intersect the earth's surface. The locii of the intersection points after the secondary forward scatter are sets of smooth arcs, the geographic co-ordinates of which can be obtained from equations (43) and (44).

It should be possible to trace all such ray paths numerically, employing a digital computer. Subsequent analysis would establish whether the mechanism offers a feasible explanation of certain anomalous VHF transequatorial propagation which has been observed over experimental paths.

REFERENCES

No.	Author	Title
1	Dyce, R.B., Dolphin, L.T., Leadabrand, R.L. and Long, R.A.	"Aurora-like radar echoes observed from 17^{o} latitude". J. Geophys. Res., 64, p 1815, November 1959
2	Bowles, K.L., Cohen, R., Ochs, G.R. and Balsley, B.B.	"Radio echoes from field-aligned ionization above the magnetic equator and their resemblance to auroral echoes". J. Geophys. Res., 65, p 1853, June 1960
3	Booker, H.G.	"A theory of scattering by non-isotropic irregularities". J. Atmos. Terr. Phys., 8, p 204, 1956
4	Leadabrand, R.L. and Yarbroff, I.	"The geometry of auroral communications". IRE Trans. Ant. Prop. AP-6, p 80, January 1958
5	Millman, G.H.	"The geometry of the earth's magnetic field at ionospheric heights". J. Geophys. Res., 64, p 717, July 1959
6	Millman, G.H.	"Field-aligned ionization scatter geometry". NATO-AGARD/EPC Symposium on "Scatter Propagation of Radio Waves", Sandefjord, Norway, August 1968
7	Jensen, D.C. and Cain, J.C.	"An interim geomagnetic field". J. Geophys. Res., 67, p 3568, August 1962

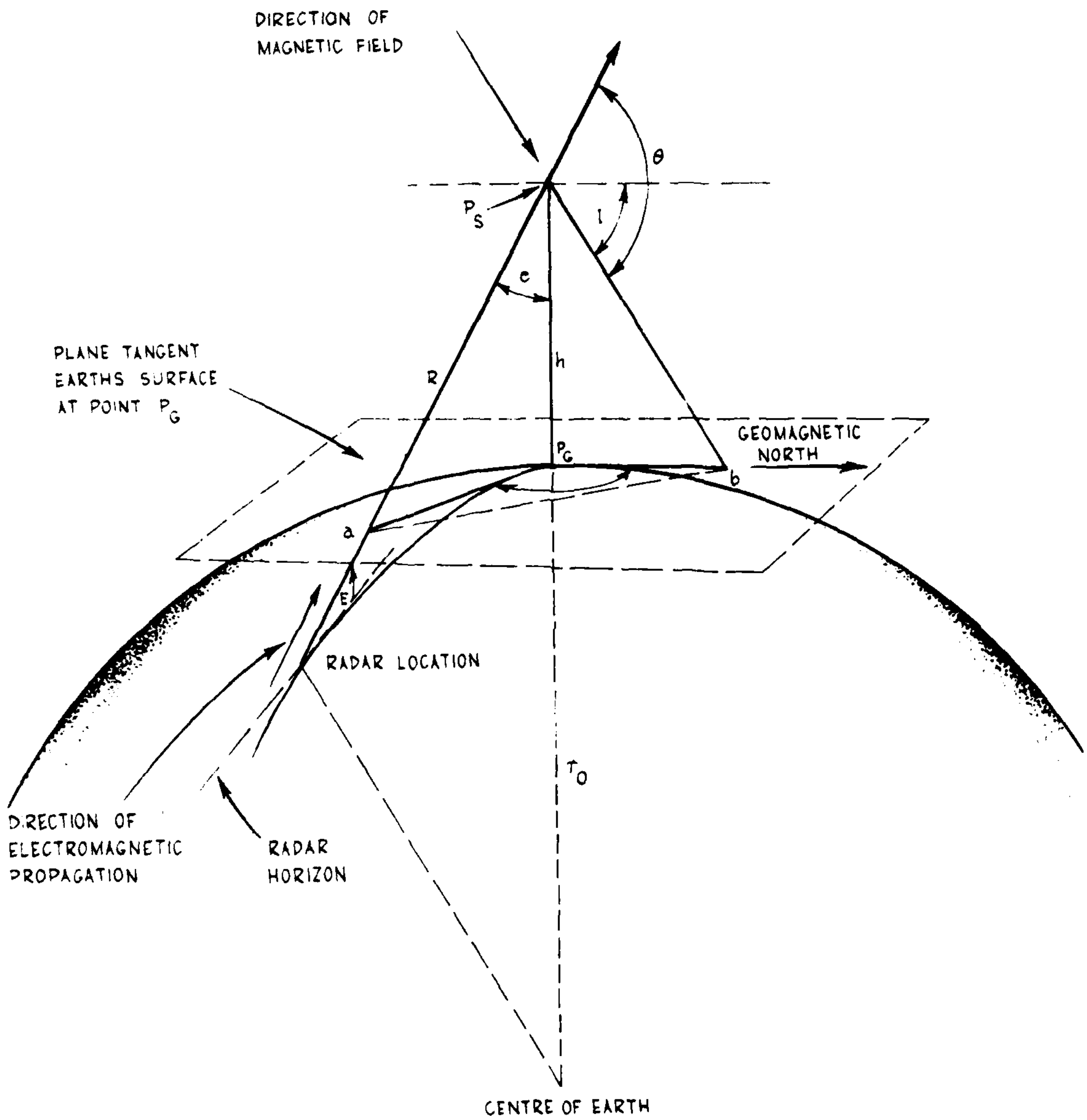

Figure 1. Propagation angle, geometric configuration (ref.5)

ERL-0158-TR
Figure 2

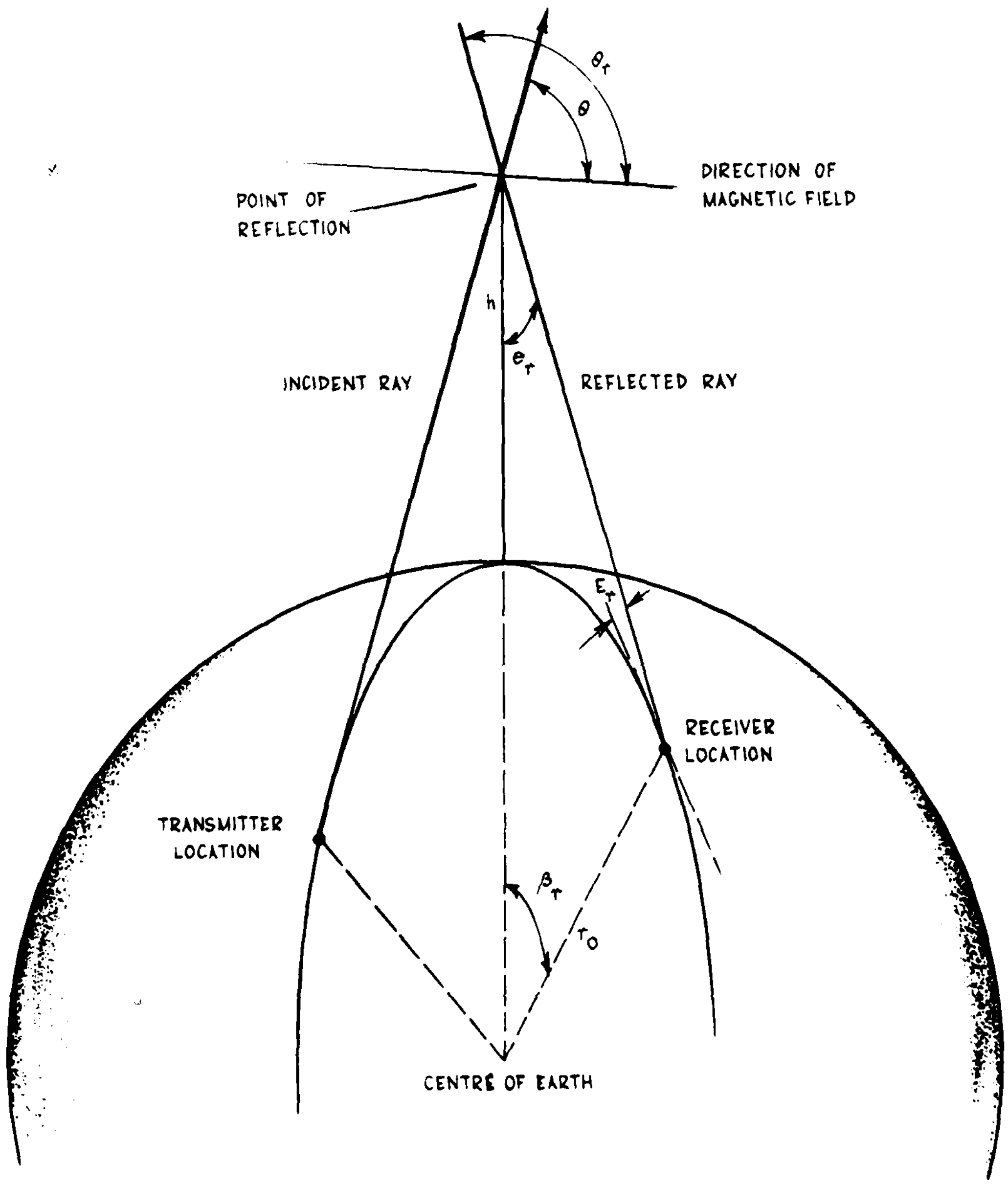

Figure 2. Auroral scattering geometry (ref.6)

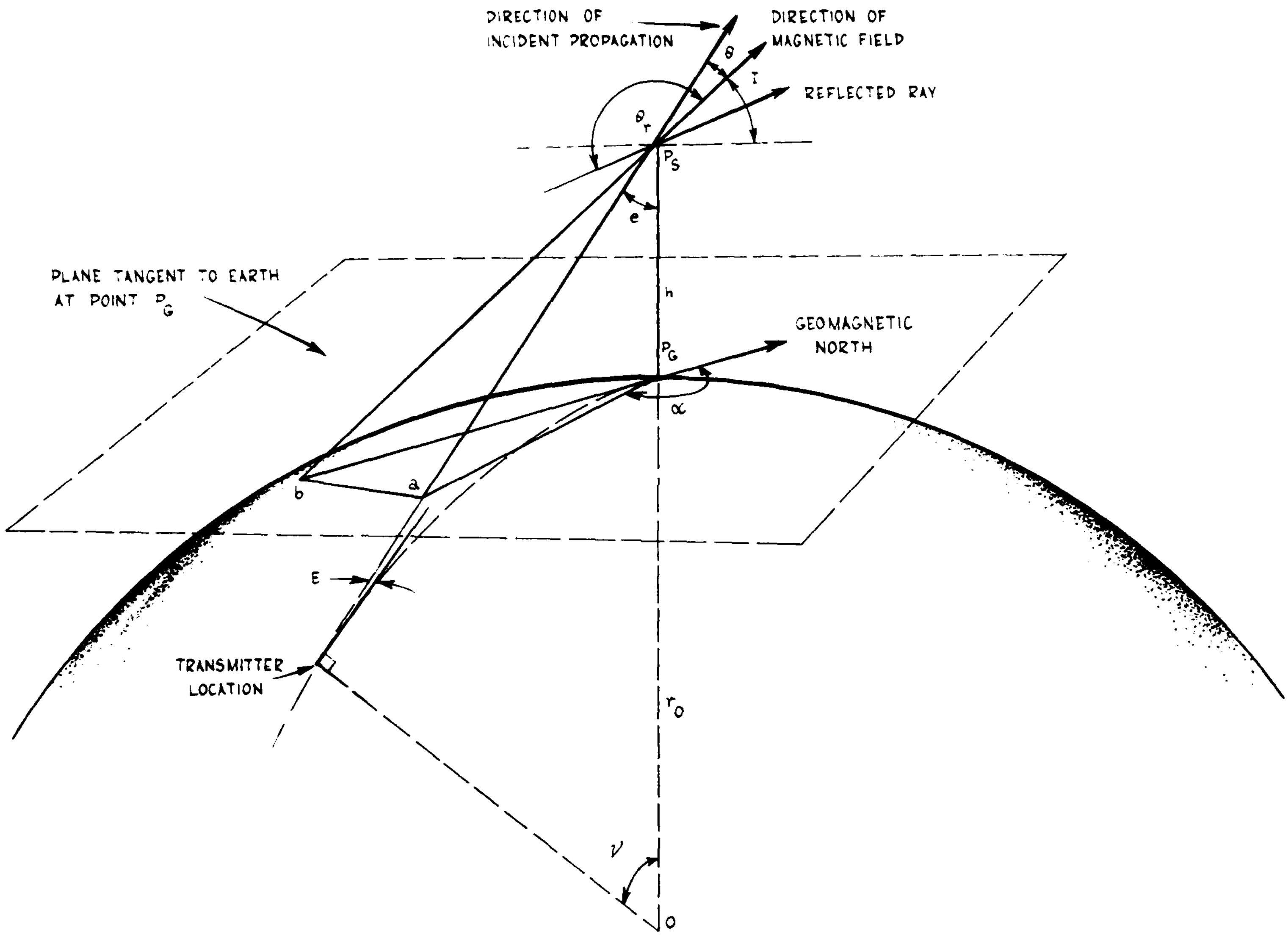

Figure 3. Scatter geometry in the southern geomagnetic hemisphere

ERL-0158-TR
Figure 4

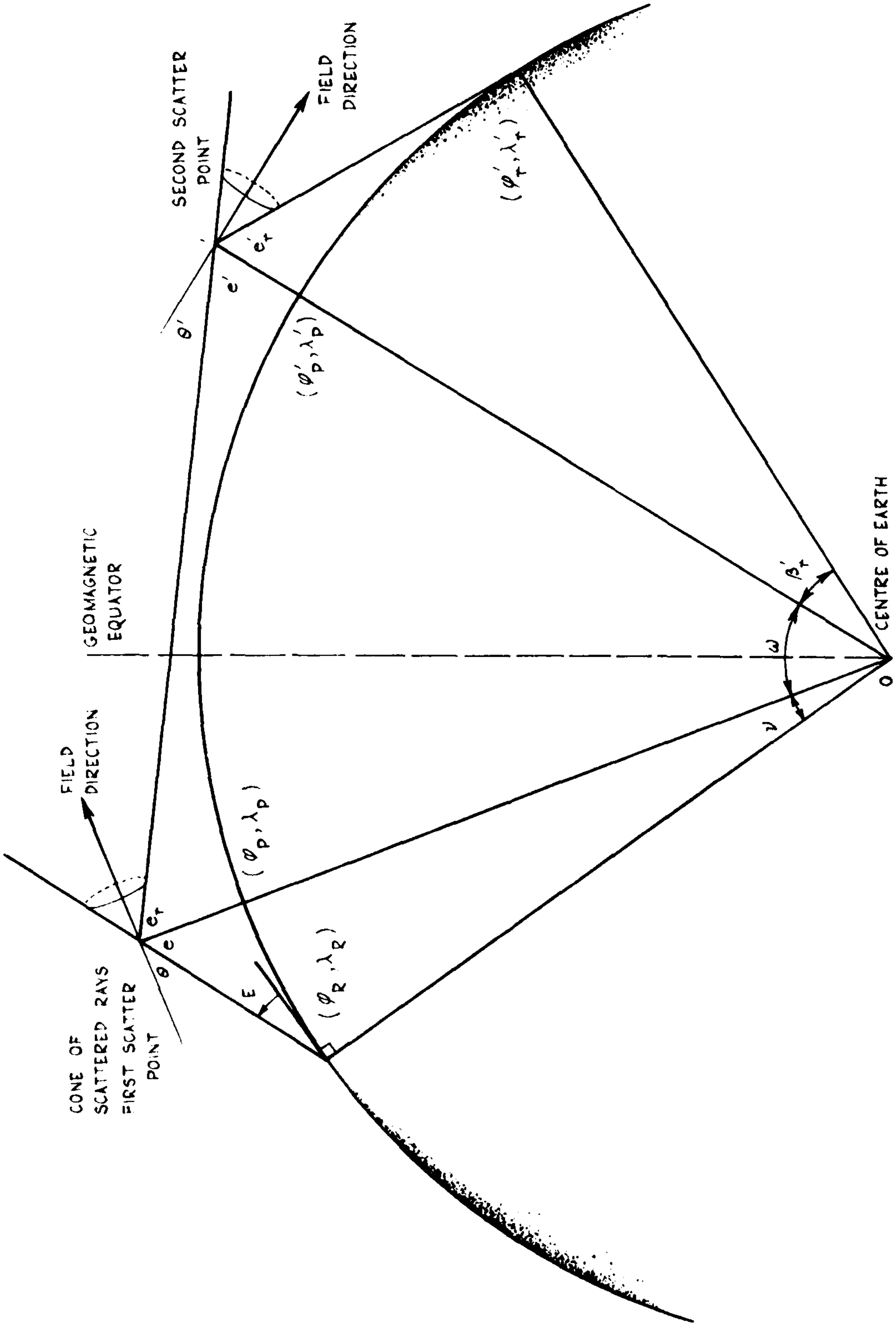

Figure 4. Transequatorial Scatter Geometry

DISTRIBUTION

EXTERNAL	Copy No.
In United Kingdom	
Defence Scientific & Technical Representative, London	No copy
British Library Lending Division, Boston Spa, Yorkshire	1
Institution of Electrical Engineers, Hitchin Herts	2
Appleton Laboratory, Ditton Park, Slough, Bucks	3
In United States of America	
Counsellor, Defence Science, Washington	No copy
Defence Research and Development Attache, Washington	4
National Technical Information Services, Springfield, Va.	5
Cambridge Scientific Abstracts, Riverdale, Md.	6
World Data Center A for Solar Terrestrial Physics NOAA, Boulder, Colorado	7
Office of Telecommunications, Institute for Telecommunication Sciences, Boulder, Colorado	
(Attention: Mrs M. Leftin)	8
ARCRL(CRMPLA), Stop 29, L.G. Hanscom Field, Bedford, Mass.	
(Attention: Exchange Librarian)	9
Stanford Research Institute, Menlo Park, California	
(Attention: Dr D.L. Nielson)	10
Dr N.C. Gerson, Trapolo Road, South Lincoln, Mass.	11
The Director, Defence Communications Agency, Washington	
(Attention: Code 513, Mr S.E. Probst)	12
South West Research Institute, San Antonio, Texas	
(Attention: Mr W. Sherrill)	13
In Canada	
Communications Research Centre, Box 490, Terminal A, Ottawa 2, Ontario, Canada	14
In Federal Republic of Germany	
Fernmeldetechnisches Zentralamt, FGR D33, 61 Darmstadt am Kavalleriesand 3	15
Institut fur Ionospharen Physik, Max Planck Institut fur Aeronomie, 3411 Lindau (Postfach 20)	
(Attention: Dr Moller)	16

	Copy No.
Ionospharen Institut, 7814 Breisach am Phein	17
In New Zealand	
Dominion Physical Laboratory, Private Bag, Lower Hutt, Wellington	18
Officer-in-Charge, Geophysical Observatory, Department of Scientific and Industrial Research, PO Box 2111, Christchurch	19
In Papua New Guinea	
University of Papua New Guinea, Department of Physics, PO Box 4820, University Post Office	20
In Asia	
The Radio Research Laboratories, 2-1 Nukui-Kitamachi, 4-Chome Koganei-shi, Tokyo, 184 Japan	
(Attention: Dr N. Wakai, Chief, Radio Wave Division)	21 - 22
(Attention: Dr I. Kuriki, Radio Wave Division)	23
Yamagawa Radio Wave Observatory, 2719, Narikawa, Yamagawa-Town, Kagoshima-Ken, Japan 891-05	24
In Australia	
Chief Defence Scientist	25
Deputy Chief Defence Scientist	26
Director, Joint Intelligence Organisation (DDSTI)	27
Controller, Projects and Analytical Studies	28
Controller, Studies Laboratories and Trials	29
Superintendent, Science and Technology Programmes	30
Superintendent, RAN Research Laboratory	31
Defence Information Services Branch (for microfilming)	32
Defence Information Services Branch for:-	
United Kingdom, Ministry of Defence, Defence Research Information Centre (DRIC)	33
United States, Defense Technical Information Centre	34 - 45
Canada, Department of National Defence, Defence Science Information Service	46
New Zealand, Ministry of Defence	47
Australian National Library	48
Superintendent, Major Projects	49
Navy Scientific Adviser	50
Air Force Scientific Adviser	51

	Copy No.
Director, Electronic Warfare (DEW) (Navy Office)	52
WgCmdr B.D. Searle, Directorate of Aircraft Requirements (AREW) (Air Office)	53
LtCol E.W. Poultney, Directorate of Military Intelligence (Army Office)	54
LtCol T.J. Richards, Directorate of Joint Operations, Plans and Training (JTS-EW)	55
Defence Library, Campbell Park	56
Library, Materials Research Laboratories	57
Library, Aeronautical Research Laboratories	58
Library, Defence Signals Directorate, Victoria Barracks, Melbourne	59
Department of Science Assistant Secretary, Ionospheric Prediction Service, PO Box 702, Darlinghurst, New South Wales	60 - 62
Physics Department, University of Queensland, St Lucia, QLD	63
Department of Physics, James Cook University of North Queensland, PO Box 999, Townsville, Queensland	64

WITHIN DRCS

Chief Superintendent, Electronics Research Laboratory	65
Superintendent, Electronic Warfare Division	66
Principal Officer, Ionospheric Studies Group	67
Mr D.F. Fyfe, Ionospheric Studies Group	68
Dr K.B. Parcell, Ionospheric Studies Group	69
Dr C. Winkler, Ionospheric Studies Group	70
DRCS Library	71 - 72
Group Clerk, Ionospheric Studies Group	73 - 89
EW Information Service	90
Spares	91 - 96

DOCUMENT CONTROL DATA SHEET

Security classification of this page: UNCLASSIFIED

1 DOCUMENT NUMBERS	**2 SECURITY CLASSIFICATION**
AR Number: AR-002-035	a. Complete Document: Unclassified
Report Number: ERL-0158-TR	b. Title in Isolation: Unclassified
Other Numbers:	c. Summary in Isolation: Unclassified

3 TITLE

FIELD-ALIGNED IONIZATION SCATTER GEOMETRY APPLIED TO TRANSEQUATORIAL PATHS

4 PERSONAL AUTHOR(S):	**5 DOCUMENT DATE:**
K.B. Parcell	August 1980
	6 6.1 TOTAL NUMBER OF PAGES: 11
	6.2 NUMBER OF REFERENCES: 7
7 7.1 CORPORATE AUTHOR(S):	**8 REFERENCE NUMBERS**
Electronics Research Laboratory	a. Task: DST 74/023
	b. Sponsoring Agency:
7.2 DOCUMENT SERIES AND NUMBER	**9 COST CODE:**
Electronics Research Laboratory 0158-TR	174844
10 IMPRINT (Publishing organisation)	**11 COMPUTER PROGRAM(S)** (Title(s) and language(s))
Defence Research Centre Salisbury	

12 RELEASE LIMITATIONS (of the document):

Approved for Public Release

12.0	OVERSEAS	NO		P.R.	1	A		B		C		D		E	

Security classification of this page: UNCLASSIFIED

Security classification of this page: UNCLASSIFIED

13 ANNOUNCEMENT LIMITATIONS (of the information on these pages):

No Limitation

14 DESCRIPTORS:

a. EJC Thesaurus Terms

Ionization
Scattering
Radio waves
Wave propagation

b. Non-Thesaurus Terms

Transequatorial propagation

15 COSATI CODES:

2014

16 LIBRARY LOCATION CODES (for libraries listed in the distribution):

17 SUMMARY OR ABSTRACT:
(if this is security classified, the announcement of this report will be similarly classified)

The mathematical description of the geometry for forward specular scattering of radio waves by field-aligned ionization irregularities has been extended to cover transequatorial ray paths. The equations presented include expressions for paths involving either one scattering point in the same geomagnetic hemisphere as the transmitter, or two scattering points, one on each side of the geomagnetic equator.

Security classification of this page: UNCLASSIFIED

END

DATE
FILMED
11-81

DTIC